energies

MDPI

Creative

Development and Verification of a Simulation Model for 120 kW Class Electric AWD (All-Wheel-Drive) Tractor during Driving Operation

Seung-Yun Baek [1,2], Yeon-Soo Kim [1,3], Wan-Soo Kim [1,2], Seung-Min Baek [1,2,*] and Yong-Joo Kim [1,2,*]

1 Department of Biosystems Machinery Engineering, Chungnam National University, Daejeon 34134, Korea; kelpie0037@gmail.com (S.-Y.B.); kimtech612@gmail.com (Y.-S.K.); wskim0726@gmail.com (W.-S.K.)
2 Department of Smart Agriculture Systems, Chungnam National University, Daejeon 34134, Korea
3 Convergence Agricultural Machinery Group, Korea Institute of Industrial Technology (KITECH), Gimje 54325, Korea
* Correspondence: bsm1104@naver.com (S.-M.B.); babina@cnu.ac.kr (Y.-J.K.); Tel.: +82-42-821-7870 (S.-M.B.); +82-42-821-6716 (Y.-J.K.)

Received: 18 April 2020; Accepted: 7 May 2020; Published: 12 May 2020

Abstract: This study was conducted to develop a simulation model of a 120 kW class electric all-wheel-drive (AWD) tractor and verify the model by comparing the measurement and simulation results. The platform was developed based on the power transmission system, including batteries, electric motors, reducers, wheels, and a charging system composed of a generator, an AC/DC converter, and chargers on each axle. The data measurement system was installed on the platform, consisting of an analog (current) and a digital part (rotational speed of electric motors and voltage and SOC (state of charge) level of batteries) by a CAN (controller area network) bus. The axle torque was calculated using the current and torque curves of the electric motor. The simulation model was developed by 1D simulation software and used axle torque and vehicle velocity data to create the simulation conditions. To compare the results of the simulation, a driving test using the platform was performed at a ground speed of 10 km/h in off- and on-road conditions. The similarities between the results were analyzed using statistical software and we found no significant difference in axle torque data. The simulation model was considered to be highly reliable given the change rate and average value of the SOC level. Using the simulation model, the workable time of driving operation was estimated to be about six hours and the workable time of plow tillage was estimated to be about 2.4 h. The results showed that the capacity of the battery is slightly low for plow tillage. However, in future studies, the electric AWD tractor performance could be improved through battery optimization through simulation under various conditions.

Keywords: electric AWD tractor; SOC level; simulation model; load measurement system; driving test

1. Introduction

Due to the increasing oil consumption of agricultural machinery and the seriousness of the pollution caused by diesel engines [1,2], the field of agricultural machinery has been actively researching electric drive type power transmission systems [3–6]. Electric tractors can reduce CO_2 emissions by up to about 70% compared to engine-driven tractors [7]. Electric drive power transmission systems can be classified into series hybrid, parallel hybrid, and electric drive [8]. In series hybrid, the engine is used only to charge the battery. Instead of the engine, the electric motor receives energy from the battery and drives the vehicle [9]. Parallel hybrids are equipped with an additional internal combustion engine to distribute power optimally by driving the vehicle with an electric motor at low loads, with

an engine at heavy loads, and simultaneously driving the vehicle at high loads [10]. The electric drive type is a method of removing the engine for battery charging and using regenerative braking for battery charging and driving the vehicle [11]. For automobiles, series hybrid and parallel hybrid vehicles have been commercialized for a long time; recently, an electric drive type has also been commercialized. However, in the field of agricultural tractors, the electric drive power transmission method is less commercialized compared to the conventional diesel engine tractor. High-torque driving motor technology is not yet suitable for application in series hybrid to a tractor. The energy conversion efficiency of an electric motor varies with load, making it difficult to maintain optimum efficiency [12]. The parallel hybrid type struggles to properly distribute power because the driving motor must perform power generation and torque assist according to load fluctuations generated during operation to efficiently distribute power [13]. In addition, the electric drive type requires expensive and large-capacity batteries [14] because agricultural operations must be performed using only a battery without an engine.

To overcome the limitations of the high-torque electric motor, electric drive technology has been studied for electric all-wheel-drive (AWD) vehicles in which four motors are mounted on the drive shaft [15]. Electric AWD can easily be applied using an electric motor with a small torque capacity. A separate engine can be installed for charging the battery, which minimizes the battery capacity. Therefore, AWD technology can replace a high-power engine with four electric motors, which can continuously perform high-torque operations by charging the battery through the additional engine.

The simulation model for the AWD platform was verified to improve tracking performance [16], energy efficiency, and steering performance [17]. The AWD platform controller algorithm was developed to improve steering performance [18] and ride comfort [19]. Research on electric AWD technology is active in the automotive field, but research on agricultural machinery such as tractors is lacking. Most AWD platforms use one motor to divert power to each axle; research is needed that applies four motors to a tractor. Since the electric AWD tractor directly drives the axle using a motor, the capacities of the electric motor and the battery must be verified. In the automotive field, actual vehicle tests were conducted to verify the design of electric drive AWD systems and component parts. However, repeating the actual vehicle test is expensive and time-consuming [20]. To solve this, the research trend is to verify the platform using 1D simulation programs such as Simcenter AMESim (ver. 16, Siemens, Munich, Germany) and SimulationX (ver. 4.0, ESI ITI GmbH, Dresden, Germany).

A dynamic model of a hybrid vehicle in AMESim was used to develop a coupling device [21], predict the driving performance [22], optimize the torque control strategies [23] and the design for a dual clutch transmission [24], and predict the shock during mode shifting and riding [25]. Hybrid vehicle models were developed using SimulationX to evaluate component and hybrid control strategies for optimizing the engine power of the hybrid system [26], to review the dynamic characteristics of the power coupling device [27], and to verify and calibrate the control algorithms for electric and hybrid vehicles [20]. In previous studies, electric drive systems were simulated using programs for specification review and performance prediction before actual vehicle development. This is because accurate performance evaluation is difficult using only simulation models. Therefore, we aimed to develop a prototype of an electric AWD tractor and simulation model and verified the model by comparing the results of the simulation with those of the actual vehicle test. To verify the simulation model, we compared the axle torque and the charging/discharging performance of the battery according to load conditions. The rate of change for SOC (state of charge) level can be predicted through the torque generated on the axle, and the available time for agricultural operation of the electric AWD tractor can be estimated through the rate of change for the SOC level.

This study was basic research on the development of an electric AWD tractor, and the simulation model was developed and verified through an actual platform. The goals of the research were to (1) develop an electric AWD tractor based on power transmission systems; (2) develop a simulation model that reflects the specifications of the parts of an electric AWD tractor; (3) verify the simulation model

through comparison of measured data with simulation results by conducting a driving test; and (4) develop a reliable simulation model that can be used to develop and supplement electric AWD tractors.

2. Materials and Methods

2.1. Concept of Electric AWD Tractor

Figure 1 depicts the composition of an electric AWD tractor and the power flow of an AWD system. Power transmission systems of electric AWD tractors consist of batteries, electric motors, reducers, wheels, and a charging system, composed of generators, AC/DC converters, and chargers. The platform was developed based on power transmission systems, and the axle must be composed of a combination of a motor and a speed reducer to cope with the high loads generated during work [15]. The capacities of the battery and generator were selected so that the motor could be supplied with constant power by considering the electric tractor's farming time of 6 h [28]. The four AWD systems are driven independently, which reduces the turning radius and improves the ease of slip control [29]. The electric motor operates by being supplied with energy from a battery and a generator, and the torque output from the motor is transmitted to the wheel through two reducers. Each control unit is configured to communicate via CAN (controller area network). The function of the AWD was developed by installing electric motors, reducers, and wheels with the same specifications on each axle. The electric systems basically consisted of a plug-in hybrid electric vehicle (PHEV) system that uses rechargeable batteries to supply electrical energy continuously.

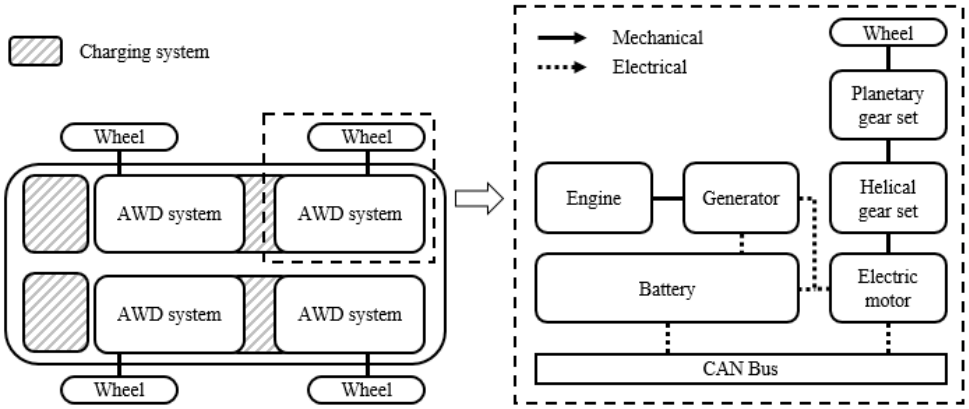

Figure 1. Schematic diagram of the power flow for the electric all-wheel-drive (AWD) tractor.

2.2. Development of Electric AWD Tractor

The electric AWD tractor was developed by combining selected electric and mechanical components for each axle, as shown in Figure 2. The total weight and dimensions were 7430 kg and 5500 × 2500 × 1950 mm (length × width × height), respectively. The weight and dimensions of a conventional tractor of the same class are 7125 kg and 4855 × 2450 × 3095 mm, respectively, so the electric AWD tractor has specifications similar to a conventional tractor. Table 1 shows the components and specifications of the electric AWD tractor. The battery type adopted was $LiFePO_4$ because it can cope with the high power output of the electric motor during operation and has a long life cycle [30]. To stably cope with the high torque of the axle generated in the harsh farming environment, the battery had a capacity of 14.6 kWh, a rated voltage of 70.4 V, and a of 2 C. It was connected to each electric motor and generator. The C-rate was selected to ensure no damage occurred to the battery when a load higher than the rated power of the motor occurred. The generators (GENEX ST15000, Honda, Tokyo, Japan) with a gasoline engine and AC/DC converter were added to supply electrical energy to batteries for continuous charging during operation. The selected rated output of the generator was 13.5 kW, considering overcharging of the battery. The battery was charged with the current generated from the generator through the converter and charger. The selected rated power of the converter was 15 kW, which was similar to

the output of the generator to increase efficiency. The maximum output current of the charger was selected as 50 A considering the safety of battery charging. The converter and charger were selected considering the input current for charging the battery and the safety of the output of the generator. Four electric motors were used to replace the engine of a conventional tractor to cope with the high load during the agricultural work. Electric motors (1238-6501 AC-34, Curtis, New York, NY, USA) were selected as an easy-to-obtain product in Korea; the maximum torque and rotational speed were 119.7 Nm and 8000 rpm, respectively. We selected the motor considering the maximum power and the rated power to develop a 120 kW class tractor. The maximum and rated powers of each electric motor were about 37 and 30 kW, respectively. To increase the torque generated on the axles during tractor operation, reducers were installed on each motor output shaft. The planetary gear reducer used an existing knuckle arm to facilitate tire mounting for the tractor, and the gear ratio was about 12.05. The helical gear reducer was selected as 4.3 to increase the torque with the planetary gear reducer, and the gear ratio considered the maximum torque generated during agricultural operations. For the wheels, we selected 380/85R24 agricultural wheels (AGRIMAX RT 855, BKT, Gujarat, India), mainly used for front wheels for a large tractor to ensure the traction and ground speed of the platform.

Figure 2. Photo of the configuration of the electric AWD tractor.

Table 1. Specifications of the electric AWD tractor and charging system.

Item			Specification
Electric AWD tractor	Length × Width × Height (mm)		5500 × 2500 × 1950
	Weight (kg)		7429
	Electric motor	Max. torque (Nm)	119.7
		Max. rotational speed (rpm)	8000
		Max. power (kW)	37
	Battery	Capacity (kWh)	14.6
		Type	$LiFePO_4$
		Voltage (V)/C-Rate (C)	70.4/2
	Reducer	Planetary gear ratio	12.05
		Helical gear ratio	4.3
	Tire		380/85R24
Charging system	Generator	Rated power (kW)	13.5
	Converter	Rated power (kW)	15
	Charger	Max. output current (A)	50

2.3. Simulation Model

The power transmission system and the control system of the electric AWD tractor were developed using SimulationX (ver. 4.0, ESI ITI GmbH, Dresden, Germany). The simulation model consisted of a mechanical model, electrical model, and control model, as shown in Figure 3. Each model reflected the actual specifications of the components. The motor model reflected the torque and rotational speed (T-N) curve provided by the manufacturer, and the battery model reflected the specifications of the capacity and voltage. The output according to the rated rotational speed was input to the generator model, and each gear ratio was input to the reducer models. The tire model was configured to be the same as the actual driving condition of the platform through input of the slip ratio for each soil condition [31]. By inputting the load data between the reducer and the tire model, the output power of the electric motor was determined. The battery SOC level changed according to the power of the electric motor during simulation.

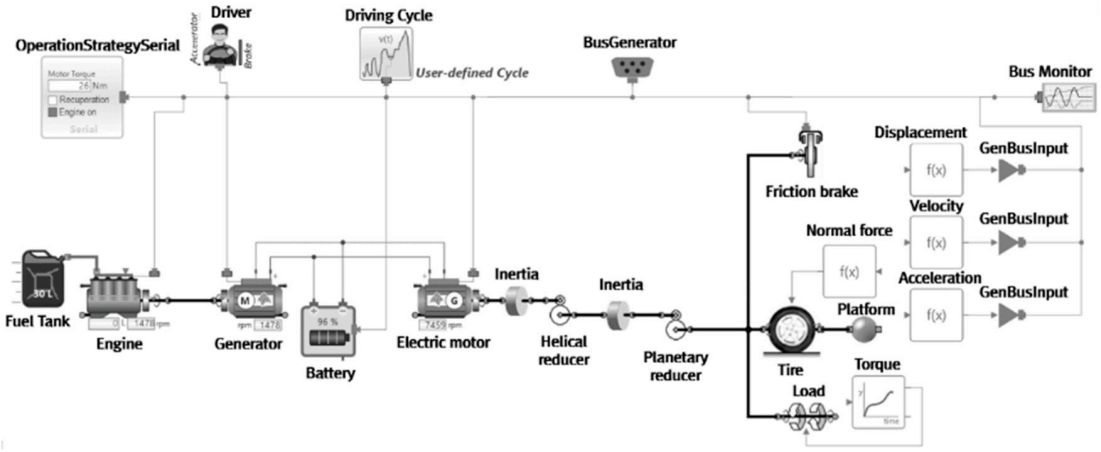

Figure 3. Simulation model for power transmission system of the electric AWD tractor using SimulationX (reproduced from [7]).

2.3.1. Mechanical Model

The mechanical model consisted of an electric motor, reducers, and tire. The axle load was input from the input torque model configured between the reducer and the tire, and the electric motor model was configured to output the motor torque considering the input load and the gear ratio of reducers. The motor torque is shown in Equation (1), which considers the air-gap torque, acceleration torque, and friction torque. Under constant voltage conditions, the current of the motor that has the most influence on the SOC is shown in Equation (2), and the torque proportional to the current is shown in Equation (3) using the gear ratio. The tire model represents wheel–road and estimates slip values at two speeds, and assigns coefficients of friction according to the prescribed slip characteristics [32].

$$T_{motor} = T_e - T_a - T_l, \tag{1}$$

where T_{motor} is motor torque (Nm), T_e is air-gap torque (Nm), T_a is acceleration torque (Nm), and T_l is motor friction torque (Nm).

$$P_{motor} = V_{in} I_{in} = \frac{2\pi \mathrm{T}_{motor} \mathrm{N}_{motor}}{60,000}, \tag{2}$$

where P_{motor} is motor power (kW), V_{in} is supply voltage (V), I_{in} is supply current (mA), T_l is motor friction torque (Nm), and N_{motor} is rotational speed of motor (rpm).

$$T_o = T_{in} \gamma_{reducer}, \tag{3}$$

where T_o is the output torque of the reducer (Nm), T_{in} is the input torque of the reducer (Nm), $\gamma_{reducer}$ is the gear ratio of the reducer.

2.3.2. Electrical Model

The electrical model consisted of a generator with engine and a battery. The generator was always driven so that it supplied 13.5 kW of output to the battery and electric motor, and the output of the generator was determined as shown in Equation (4). The battery applied a capacity of 14.6 kWh, and the initial SOC level was set in accordance with the test conditions. SOC level was calculated from the current output from the motor and generator [30,33], as shown in Equation (5).

$$P_{generator} = V_{in}I_{in} \ (P_{generator} \geq 0), \tag{4}$$

where $P_{generator}$ is motor power (kW).

$$\mathrm{SOC(k)} = \mathrm{SOC(0)} - \frac{T}{C_n}\int_0^k (\eta I(t) - S_d)dt, \tag{5}$$

where $\mathrm{SOC}(0)$ is the battery initial SOC, $I(t)$ is the current at time t, T is the sampling period, C_n is the nominal capacity of the battery, η is the coulombic efficiency, and S_d is the self-discharging rate. For a $LiFePO_4$ battery, $\eta > 0.994$ at room temperature and the self-discharging rate is about 5% per month.

2.3.3. Simulation Condition

The driving cycle model represents the preset vehicle velocity and vehicle acceleration. Vehicle velocity was calculated based on motor rotational speed and tire diameter, as shown in Equation (6) [34]. The operation strategy serial model operates the generator according to the setting range of the SOC level of the battery. The charging range of the SOC level was set to the condition that the generator is always driven. All models were connected via a bus system, and the models interacted according to input conditions. The time steps of the simulation were set to 35 s and 40 s in the off-road and the on-road condition, respectively, to match the load measurement time during the driving test.

$$V_{platform} = \frac{N_{motor}}{\gamma_{reducer}} \times \frac{60}{1000} \times d_{tire} \times \pi, \tag{6}$$

where $V_{platform}$ is velocity (km/h), N_{motor} is the rotational speed of the motor (rpm), $\gamma_{reducer}$ is the gear ratio of the reducer, and d_{tire} is the tire diameter (m).

2.4. Verification of Electric AWD Tractor

2.4.1. Load Measurement System

The load measurement system was developed and installed on an electric AWD tractor for measuring real-time data during operation, as shown in Figure 4. The current sensors (LF-1005S, LEM USA Inc., Milwaukee, WI, USA) and CAN logging system were installed to measure current and rotational speed of electric motors and voltage of batteries for calculating axle torque. The current sensors used in this study were installed between each battery and controller of the electric motor, generating a coil magnetic field according to the current flow and recognizing the current generated by the magnetic field detecting of the hall sensor up to 1000 mA. The SOC level was measured using the CAN logging system connected to a battery management system (BMS). A data acquisition device (QuantumX MX840, HBM, Darmstadt, Germany) was installed to acquire and transfer the signals from the current sensors and the CAN logging system to the laptop computer. The accuracy classes of the data acquisition device ranged from 0.05% to 0.1% depending on the sensor technology. Two 24-bit analog input channels with a sampling rate of 300 Hz per channel were used to acquire the current,

and four digital input channels with a sampling rate of 300 Hz per channel were used to measure the CAN data. The measured signals were transmitted and saved on the laptop computer through the signal processing program CATMAN (ver. 3.1, HBM, Darmstadt, Germany).

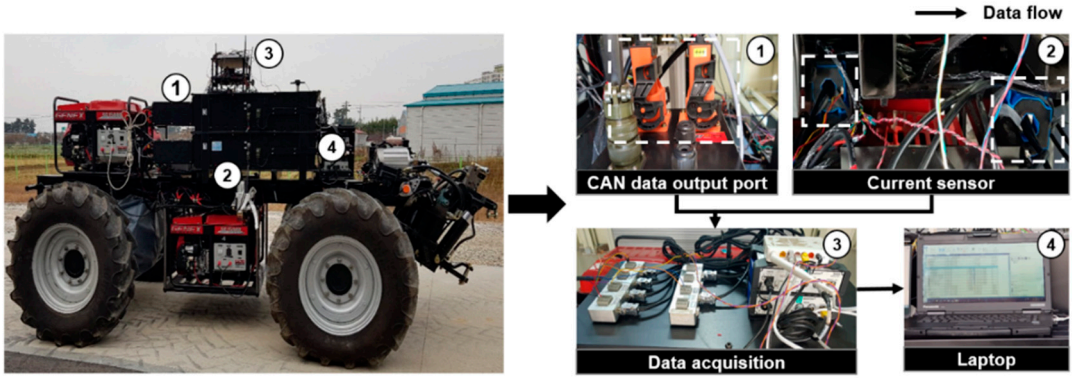

Figure 4. Load measurement system and data flow of electric AWD tractor.

2.4.2. Test Procedure

We conducted driving tests to measure data for calculating axle torque on a test track (Latitude: 35°56′08.5″ N, Longitude: 126°55′33.1″ E) in Iksan-si, Jeollabuk-do province, Republic of Korea. Driving tests were conducted at a ground speed of 10 km/h considering the working speed of a tractor, which is the standard used in the tractor design [35] under off-road (field) and on-road (asphalt) conditions, as shown in Figure 5. The driving test was conducted with the generator always running during all operations and the generator's gasoline fuel tank was filled with 30 L. The driving test was conducted through a wireless controller that controlled the speed of the four motors. The platform traveled approximately 45 m for 25 s in off-road conditions and 80 m for 35 s in on-road conditions at 10 km/h. Data measurement was performed in off-road and on-road conditions for 35 s and 40 s, respectively, and the measurement time included a stop section of about 10 s before and after the driving test.

(**a**) (**b**)

Figure 5. Photos of driving operation of electric AWD tractor under (**a**) off-road and (**b**) on-road conditions.

Figure 6 shows the overall test procedure as a flow chart. The current and rotational speed of electric motors and voltage of batteries measured during the test were converted into torque using the current–torque characteristic curve. The current–torque characteristic curve was provided by the motor manufacturer, and the output torque of the motor was calculated according to voltage, motor rotation speed, and current. The calculated torque was converted to axle torque by applying gear ratios of 4.3 and 12.05. The calculated torque and velocity of the vehicle were used as input conditions for the simulation. The measured data and simulation results of the axle torque and SOC level of the

battery were compared through simulation, and the similarities between the two results were verified using t-test calculated with IBM SPSS Statistics software (SPSS 25, IBM Corp., Armonk, NY, USA).

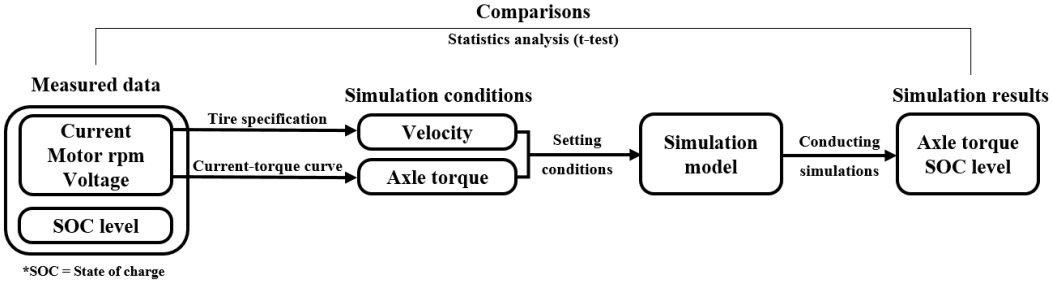

Figure 6. Flow chart of the test procedure for development and verification of electric AWD tractor.

3. Results

3.1. Axle Torque

The axles of the electric AWD tractors had the same size of wheels and same weight distribution ratio, so the output torque of the motors did not vary significantly from axle to axle. However, when the steering of the vehicle adopts skid steering [16], a difference occurs in the output torque of the motors located on the left and right sides, so the simulation model was verified using data from each axle. Figure 7 provides a comparison of the measured and simulated results of the averaged axle torque at a ground speed of 10 km/h in off-road conditions. The axle torque was considerably affected by the ground speed in off-road conditions. In addition, the axle torque has been shown to vary not only by soil irregularities, but also by steering for straight driving. The axle torque peaked as the electric motor accelerated, and then changed due to repeated deceleration and acceleration for steering. The maximum and average measured torques of the left axle were 6847.4 and 3771.8 Nm, respectively, and 6345.5 and 2580.1 Nm, respectively, for the right axle. The simulation results showed similar trends in all sections, but the largest differences for each axle were 1425.2 and 1850.2 Nm in the sections where the platform starts to operate and where the maximum torque occurred, respectively.

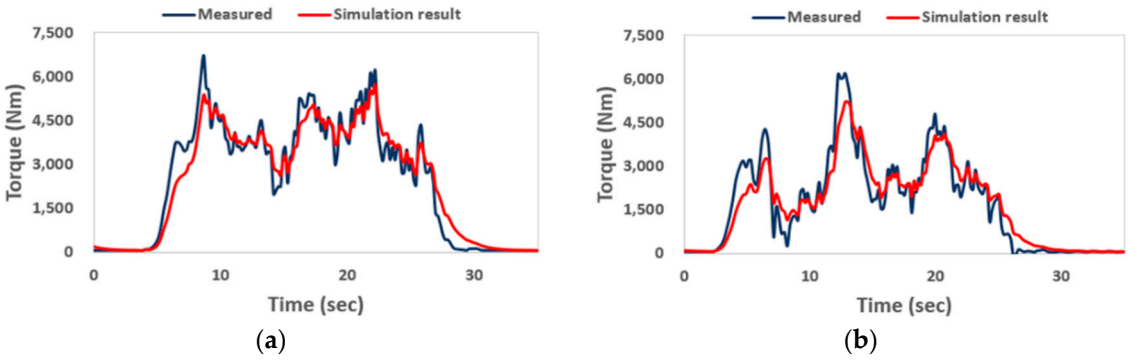

Figure 7. Comparison of averaged axle torque of (**a**) left and (**b**) right sides of the tractor for measured and simulated results at a ground speed of 10 km/h in off-road conditions.

Figure 8 provides a comparison of the measured and simulated results of the averaged axle torque at a ground speed of 10 km/h in on-road conditions. The axle torque has been shown to vary with steering for straight driving. The driving test performed in the on-road condition had a small load fluctuation compared to the off-road condition because the soil had little influence on asphalt driving. The maximum and average measured torques of the left axle were 1905.9 and 689.1 Nm, and 1644.9 and 161.7 Nm for the right axle, respectively. The minimum torques of the left and right axles were −625.0 and −732.1 Nm, respectively, by decelerating the electric AWD tractor for steering.

The simulation results showed similar trends in all sections, but the highest differences for the left and right axle were 572.9 and 581.3 Nm, respectively, in the section where the maximum torque occurred.

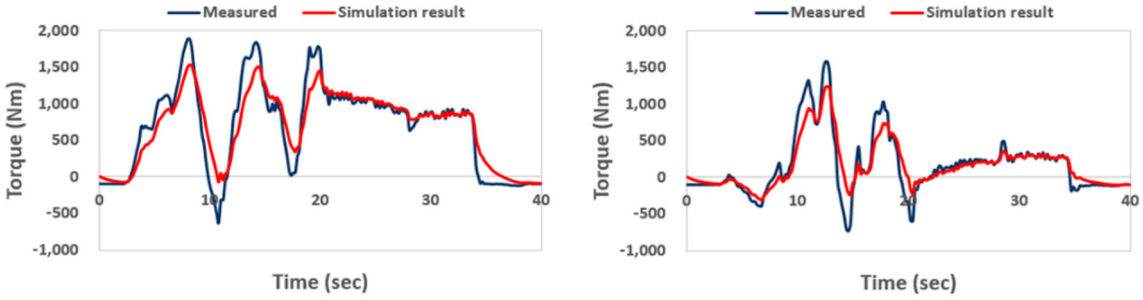

Figure 8. Comparison of averaged tractor axle torque of (**a**) left and (**b**) right sides for measured and simulated results at ground speed of 10 km/h in on-road conditions.

The simulated axle torque was smaller than the measured value in most sections. This is because the simulation analysis was performed in different conditions compared to the actual vehicle test. For example, the inertia models connected to the motor and reducer model were set to a default value because it is difficult to measure the exact value during a driving test. As the input value of the inertia model decreases, it is judged that the simulated torque of the electric motor is lower than the measured value because a lower force was required. However, it is possible to obtain more similar results by selecting the proper value of the inertia model using the inertial measurement unit (IMU). Table 2 lists the axle torque differences between the measured and simulated results based on the operation conditions. The average torques of the left and right motors were about 1800 and 1900 Nm higher in the off-road than on-road conditions, respectively. The maximum average torques of the motors were similar on the right and left sides, but the average value was about 700 Nm higher on the left side on the off-road condition. This difference was caused by the load according to the difference in the rotational speed of the left and right sides by the skid steering. The results of the t-test showed that the *p*-value was higher than 0.05 under all conditions, indicating no significant differences between the measured and simulated results of axle torque. Therefore, the simulation model was able to evaluate the axle torque of the electric AWD tractor during operation.

Table 2. Comparison of axle torque between measured and simulated results based on the operation conditions at 10 km/h.

Field Conditions	Electric Motor	Measured Axle Torque (Nm)	Simulated Axle Torque (Nm)	*p*-Value
Off-road	Left	2490.8 ± 2005.3 [1]	2497.4 ± 1865.5	0.846
	Right	1702.6 ± 1596.4	1705.3 ± 1402.5	0.941
On-road	Left	689.1 ± 601.1	687.8 ± 484.9	0.934
	Right	161.7 ± 413.0	166.3 ± 310.1	0.696

Note: [1] Average ± standard deviation.

3.2. SOC Level of Battery

The measured and simulated SOC levels were compared when the vehicle was traveling at 10 km/h. Figure 9 depicts the results in off-road conditions. The initial and final SOC levels of the battery connected to the left motor were measured at 96.30% and 96.10%, respectively, and 80.00% and 79.90% for the right motor, respectively. Simulation analysis showed that the initial and final SOC levels of the battery connected to the left motor were 96.30% and 96.11%, respectively, and 80.00% and 79.90% for the right motor, respectively. The rate of change of the SOC level during operations by driving the left motor for measured and simulated results were about 0.20% and 0.18%, respectively,

with a 0.02% difference between results. The rate of change of the SOC level by the right driving motor for measured and simulated results was similar, with a 0.10% difference between results.

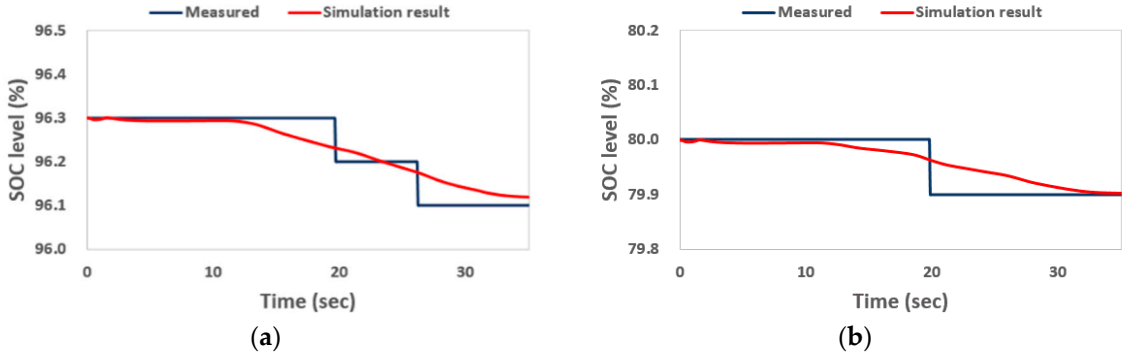

Figure 9. Comparison of averaged SOC level of (**a**) left battery and (**b**) right battery for measured and simulated results at a ground speed of 10 km/h under off-road conditions.

Figure 10 depicts the measured and simulated results of the averaged SOC level at a ground speed of 10 km/h under on-road conditions. The initial and final SOC levels of the battery connected to the left motor were measured at 97.20% and 97.00%, respectively; for the battery connected to the right motor, the measurements were 80.00% and 79.90%, respectively. Simulation analysis showed that the initial and final SOC levels of the battery connected to the left motor were 97.20% and 96.99%, respectively. For the battery connected to the right motor, these values were 80.00% and 79.89, respectively. The rate of change in the SOC level during operations by driving the left motor for the measured and simulated results were about 0.20% and 0.21%, respectively, a 0.01% difference between results. The results for the right driving motor showed a similar difference of 0.10%.

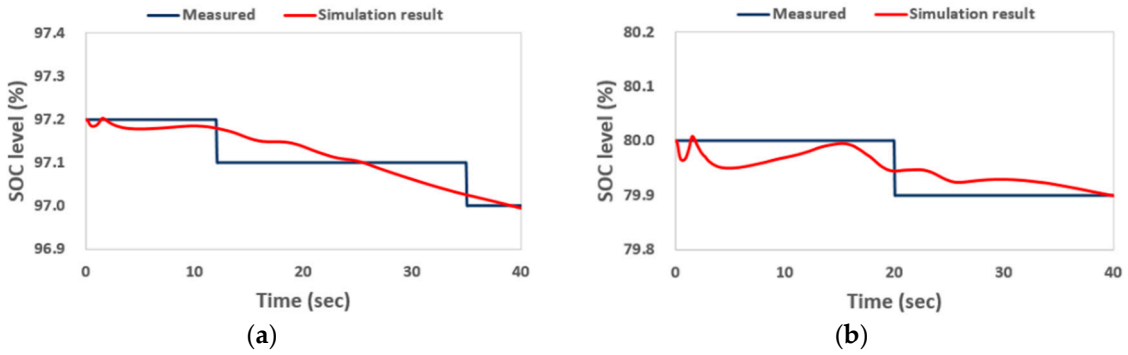

Figure 10. Comparison of averaged SOC level of (**a**) left battery and (**b**) right battery for measured and simulated results at a ground speed of 10 km/h under on-road conditions.

The SOC level is changed by the motor output, but we found that the SOC level of the battery connected to each motor did not change dramatically by continuously supplying power to the battery and motor by always driving the generator during driving operation. Table 3 provides a comparison of the SOC level between the measured and simulated results based on the operation conditions. The *t*-test results showed that there was no significant difference between measured and simulated results of the SOC level for the all battery except right battery at a ground speed of 10 km/h in off-road conditions. The *p*-value was less than 0.05 only for the right battery under off-road conditions, and there were no significant differences except for this one condition. The final variation in SOC (SOC_{fv}) was calculated using the initial and final values of the battery SOC level [3], and the SOC_{fv} was compared through measurement and simulation analysis results. Similarity was not verified in the one item in the *t*-test, but the difference in SOC_{fv} showed a similar trend. According to the low resolution power of the measurement system, the results of measurement and simulation did not match in all

sections. Due to the low resolution power, the SOC level measured through the measurement system can be checked only up to 0.1% change. Otherwise, the simulation results of the SOC level are different from the measurement results because the reduction rate appears in real time. The SOC level is expected to be more accurate compared with the higher resolution power of the measurement system. Besides, the SOC_{fv} and the average and standard deviation values of the two results showed slight differences. Therefore, the simulation model was able to evaluate the SOC level of the electric AWD tractor during operation according to the axle torque.

Table 3. Comparison of SOC level and final variation in SOC (SOC_{fv}) between measured and simulated result based on the operation conditions at 10 km/h.

Field Conditions	Battery	*t*-Test			SOC_{fv} (%)	
		SOC Level (%)				
		Measured	Simulated	*p*-Value	Measured	Simulated
Off-road	Left	96.20 ± 0.08 [1]	96.23 ± 0.06	0.400	0.20 [2]	0.18
	Right	79.95 ± 0.05	79.96 ± 0.03	2×10^{-9} *	0.10	0.10
On-road	Left	97.12 ± 0.06	97.12 ± 0.06	0.719	0.20	0.21
	Right	79.95 ± 0.05	79.95 ± 0.03	0.326	0.10	0.11

Note: * Significant difference at $p < 0.05$; [1] Average ± standard deviation; [2] $SOC_{fv} = SOC_{initial} - SOC_{final}$.

4. Discussion

The axle torque of the AWD tractor showed similar trends in all sections except when the platform started to operate or maximum torque was reached. The measured torque data tended to be similar to the simulation data, but the measured values were higher in most sections. The selection of motors and reducers for electric-powered AWD tractors needs to account for these differences, especially in the development and complementary phases. The SOC level rate of change values were similar, with a maximum error of 0.02%, but the form of decline in the graph was different given the resolution of the measurement system. The decrease rate of SOC level showed slight changes due to the continuously operated generator during driving operation. The decrease rate per minute of SOC level was about 0.3% in off-road and on-road conditions. The SOC level was not significantly different between off-road and on-road as regenerative braking occurred in on-road driving conditions [11,36]. In addition, as the driving test was conducted for a short period of time, the SOC level of the battery was determined to have little influence on the output torque of the motor according to the field conditions, because it mainly used the current supplied from the generator. However, the electric AWD tractor cannot be operated only with the current supplied from the generator if the working time is prolonged.

We determined that the reduction rate of the SOC battery level changes according to current consumption by increasing the output torque of the motor during long working hours. The SOC level reduction rate is expected to be greater in off-road than on-road conditions when the driving test is conducted without regenerative braking. The workable time of the electric AWD tractor was estimated to be about 6 h based on the axle torque generated during driving operation. The platform can travel for about 6 h at a speed of 10 km/h, and estimated driving range is calculated as approximately 60 km according to the reduction rate of the SOC level and workable time. Estimated driving range is expected to be longer due to battery charging by regenerative braking in the actual driving environment. Since the tractor was designed based on the results of research on driving operation [37–39], available time for work was predicted through torque comparison by plow tillage using the existing research. The torque data were compared with off-road driving data because it is difficult to compare the average value given the negative value generated by regenerative braking during driving operation under on-road conditions. Tillage is the agricultural preparation of soil by mechanical agitation of various types, such as digging, stirring, and overturning [40], and it is the harshest operation, accounting for over 60% of engine power [41]. The average axle torques of the driving operation and plow

tillage were reported to be 1452.1 and 3680.3 Nm, respectively [15]. The estimated torque of each axle for plow tillage was 3221.5 Nm and the workable time was predicted to be 2.4 h, as summarized in Table 4. The average torque generated on the axle during plow tillage is about 2.5 times higher than the averaged torque during driving operation [7], and the workable time for plow tillage using electric AWD tractors is estimated to be about 40% lower than workable time for driving operation. The average working time of the tractor is six hours in Korea, and it can be assumed that the morning and afternoon work are performed for three hours each. The battery performance of the electric AWD tractor developed in this study was lower than three hours; however, the working time can be extended by increasing the capacity of the battery and by fast charging during the break in the middle of the workday.

Table 4. Estimated torque and workable time for electric AWD tractor according to torque ratio of operations.

Agricultural Operation	Torque Ratio	Estimated Torque (Nm)	Estimated Time (Hours)
Plow tillage	2.5 [1]	3221.5 [2]	2.4

Note: [1] Ratio of axle torque during driving operation; [2] Averaged torque applying torque ratio to driving data.

The electric AWD tractor was developed considering the load generated during operation, the required output, and the workable time. The developed system has the advantage of being applicable to various fields including construction machinery, depending on the selection of electric motor and reducer according to the output and torque, and the capacity of the battery and generator considering the usage time and discharge rate. The platform has the required output according to the combination of the electric motor and the reducer, and the usage time and the size of the platform are determined by selecting the proper capacity of the battery and the generator. The developed simulation model consists of all components including electric motors, reducers, batteries, and generators, and it is also possible to simulate and analyze the AWD platforms with different outputs and sizes by modifying each performance map and specifications. However, the simulation model can be utilized through partial modification of the simulation model in the case of a similar AWD platform, and it is judged that there are limitations in the simulation and analysis of the AWD platforms with different systems. In future studies, simulations and field tests including tillage should be performed and verified under a variety of conditions to optimize the electric-powered tractor components.

5. Conclusions

In this study, an electric AWD tractor was developed based on a power transmission system. A simulation model reflecting the specifications of this electric AWD tractor was developed and verified using measured data from driving tests conducted under off-road and on-road conditions. The measured data were converted to torque using equations and were used for simulation conditions. A comparison of the simulation analysis results with the measured data showed that the torque generated on the axle was similar in value and shape, and we found no significant differences in the statistical analysis results. Although the SOC level showed a significant difference in the statistical analysis results, the rate of change per minute, and the SOC_{fv}, the simulation results were considered to be reliable. The axle torque is closely related to the SOC level because it is proportional to the current supplied from the battery to the electric motor. As the measured data for both factors matched the simulation results, we determined that the operating time of the platform can be estimated through simulation. The workable time of the electric AWD tractor was estimated through simulation models and existing research data. As a result of simulation, the workable time for plow tillage using the electric AWD tractor was estimated to be about 2.4 h. The results are less than the target hours (three hours) of work. In future studies, performance could be improved through battery optimization through a simulation.

Author Contributions: Conceptualization, S.-Y.B. and Y.-J.K.; methodology, S.-Y.B. and W.-S.K.; software, S.-Y.B. and Y.-S.K.; validation, S.-Y.B.; writing—original draft preparation, S.-Y.B.; writing—review and editing, S.-Y.B., S.-M.B. and Y.-J.K.; supervision, Y.-J.K.; project administration, Y.-J.K. All authors have read and agreed to the published version of the manuscript.

Funding: This work was supported by the Industrial Strategic Technology Development Program (10083590, Development of construction and agricultural robot platform technology with autonomous system for all-wheel drive of 100kW class) funded by the Ministry of Trade, Industry and Energy (MI, Korea).

Conflicts of Interest: The authors declare no conflict of interest.

References

1. Lee, D.H.; Choi, C.H.; Chung, S.O.; Kim, Y.J.; Inoue, E.; Okayasu, T. Evaluation of tractor fuel efficiency using dynamometer and baler operation cycle. *J. Fac. Agric. Kyushu Univ.* **2016**, *61*, 173–182.
2. Chen, Y.; Xie, B.; Mao, E. Electric Tractor Motor Drive Control Based on FPGA. *IFAC-PapersOnLine* **2016**, *49*, 271–276. [CrossRef]
3. Lee, D.H.; Kim, Y.J.; Choi, C.H.; Chung, S.O.; Inoue, E.; Okayasu, T. Development of a parallel hybrid system for agricultural tractors. *J. Fac. Agric. Kyushu Univ.* **2017**, *62*, 137–144.
4. Kang, E.; Pratama, P.S.; Byun, J.; Supeno, D.; Chung, S.; Choi, W. Development of Super-capacitor Battery Charger System based on Photovoltaic Module for Agricultural Electric Carriers. *J. Biosyst. Eng.* **2018**, *43*, 94–102.
5. Azwan, M.B.; Norasikin, A.L.; Sopian, K.; Abd Rahim, S.; Norman, K.; Ramdhan, K.; Solah, D. Assessment of electric vehicle and photovoltaic integration for oil palm mechanisation practise. *J. Clean. Prod.* **2017**, *140*, 1365–1375. [CrossRef]
6. Moreda, G.P.; Muñoz-García, M.A.; Barreiro, P. High voltage electrification of tractor and agricultural machinery—A review. *Energy Convers. Manag.* **2016**, *115*, 117–131. [CrossRef]
7. Baek, S.Y.; Kim, W.S.; Kim, Y.S.; Kim, Y.J.; Park, C.G.; An, S.C.; Moon, H.C.; Kim, B.S. Development of a Simulation Model for an 80 kW-class Electric All-Wheel-Drive (AWD) Tractor using Agricultural Workload. *J. Drive Control* **2020**, *17*, 27–36.
8. Ko, J.W.; Ko, S.; Park, Y.C. A Study on Battery Performance of a Motor Driven Local Transportation Vehicle. *J. Korean Soc. Mar. Eng.* **2012**, *36*, 430–436. [CrossRef]
9. Liu, W.; He, H.; Wang, Z. A Comparison Study of Energy Management for A Plug-in Serial Hybrid Electric Vehicle. *Energy Procedia* **2016**, *88*, 854–859. [CrossRef]
10. Park, J.K. *Design of Parallel Hybrid Tractor and Evaluation of Charge/Discharge Performance*; Sungkyunkwan University: Seoul, Korea, 2013.
11. Zhao, W.; Wu, G.; Wang, C.; Yu, L.; Li, Y. Energy transfer and utilization efficiency of regenerative braking with hybrid energy storage system. *J. Power Sources* **2019**, *427*, 174–183. [CrossRef]
12. Liu, M.; Xu, L.; Zhou, Z. Design of a Load Torque Based Control Strategy for Improving Electric Tractor Motor Energy Conversion Efficiency. *Math. Probl. Eng.* **2016**, *2016*, 2548967. [CrossRef]
13. Park, Y., II; Kim, Y.J. Technology for the Agricultural Hybrid Tractor. *Auto J.* **2014**, *36*, 30–34.
14. Mousazadeh, H.; Keyhani, A.; Javadi, A.; Mobli, H.; Abrinia, K.; Sharifi, A. Evaluation of alternative battery technologies for a solar assist plug-in hybrid electric tractor. *Transp. Res. Part D Transp. Environ.* **2010**, *15*, 507–512. [CrossRef]
15. Kim, W.S.; Baek, S.Y.; Kim, T.J.; Kim, Y.S.; Park, S.U.; Choi, C.H.; Hong, S.J.; Kim, Y.J. Work load analysis for determination of the reduction gear ratio for a 78 kW all wheel drive electric tractor design. *Korean J. Agric. Sci.* **2019**, *46*, 613–627.
16. Kim, B.S. *Slip Detection and Control Algorithm to Improve Path Tracking Performance of Four-Wheel Independently Actuated Vehicles*; Hongik University: Seoul, Korea, 2019.
17. Song, H.W. *A Study on the Improvement of Energy Efficiency and Cornering Stability Performance for 4WD in-Wheel Electric Vehicle*; Sungkyunkwan University: Seoul, Korea, 2013.
18. Jeon, D.S. *Study about Skid Steer of Independent 4 Wheel Drive Vehicle*; Kookmin University: Seoul, Korea, 2008.

19. Song, C.H. *Development of Motor Control Algorithm of an All-Wheel Drive In-Wheel Electric Vehicle to Improve Ride Comfort*; Sungkyunkwan University: Seoul, Korea, 2015.
20. Klein, S.; Xia, F.; Etzold, K.; Andert, J.; Amringer, N.; Walter, S.; Blochwitz, T.; Bellanger, C. Electric-Motor-in-the-Loop: Efficient Testing and Calibration of Hybrid Power Trains. *IFAC-PapersOnLine* **2018**, *51*, 240–245. [CrossRef]
21. Zhang, D.X.; Zeng, X.H.; Wang, P.Y.; Wang, Q.N. Co-simulation with AMESim and MATLAB for differential dynamic coupling of hybrid electric vehicle. In Proceedings of the IEEE Intelligent Vehicles Symposium, Xi'an, China, 3–5 June 2009; pp. 761–765.
22. Hong, J.; Kim, S.; Min, B. Drivability development based on CoSimulation of AMESim vehicle model and simulink HCU model for parallel hybrid electric vehicle. SAE Technical Papers. In Proceedings of the SAE World Congress & Exhibition, Detroit, MI, USA, 20–23 April 2009.
23. Hwang, H.S.; Yang, D.H.; Choi, H.K.; Kim, H.S.; Hwang, S.H. Torque control of engine clutch to improve the driving quality of hybrid electric vehicles. *Int. J. Automot. Technol.* **2011**, *12*, 763–768. [CrossRef]
24. Cao, X.; Du, C.; Yan, F.; Xu, H.; He, B.; Sui, Y. Parameter Optimization of Dual Clutch Transmission for an Axle-split Hybrid Electric Vehicle. In Proceedings of the IFAC-PapersOnLine, Vienna, Austria, 4–6 December 2019; Elsevier B.V.: Amsterdam, The Netherlands, 2019; Volume 52, pp. 423–430.
25. Zeng, X.; Yang, N.; Wang, J.; Song, D.; Zhang, N.; Shang, M.; Liu, J. Predictive-model-based dynamic coordination control strategy for power-split hybrid electric bus. *Mech. Syst. Signal Process.* **2015**, *60*, 785–798. [CrossRef]
26. Wenyong, L.; Abel, A.; Todtermuschke, K.; Tong, Z. Hybrid vehicle power transmission modeling and simulation with SimulationX. In Proceedings of the 2007 IEEE International Conference on Mechatronics and Automation, ICMA 2007, Heilongjiang, China, 5–9 August 2007; pp. 1710–1717.
27. Tiantian, Z.; Sihong, Z.; Xiaoting, D. Research of Dynamic Characteristics on Power Coupling Equipment of Hybrid Electric Tractor. *Tract. Farm Transp.* **2013**, *4*, 7.
28. Korea Agricultural Machinery Industry Cooperative (KAMICO); Korean Society for Agricultural Machinery (KSAM). *Agricultural Machinery Yearbook in Korea*; Korea Agricultural Machinery Industry Cooperative and Korean Society for Agricultural Machinery: Suwon, Korea, 2019.
29. Jayaram, P.; Bharath, N.; Ahmed, R. A Novel Design for an all Terrain Custom-Built Vehicle Dynamics. *Int. J. Adv. Sci. Res. Eng.* **2018**, *4*, 186–194. [CrossRef]
30. Zhang, R.; Xia, B.; Li, B.; Cao, L.; Lai, Y.; Zheng, W.; Wang, H.; Wang, W. State of the art of lithium-ion battery SOC estimation for electrical vehicles. *Energies* **2018**, *11*, 1820. [CrossRef]
31. Kim, Y.S.; Lee, S.D.; Kim, Y.J.; Kim, Y.J.; Choi, C.H. Effect of tractor travelling speed on a tire slip. *Korean J. Agric. Sci.* **2018**, *45*, 120–127.
32. Wohnhaas, A.; Hötzer, D.; Sailer, U. Modulares Simulationsmodell eines KFZ-Antriebstrangs unter Berücksichtigung von Nichtlinearitäten und Kupplungsvorgängen.pdf. *VDI Ber.* **1995**, *1220*, 97–117.
33. Zhang, C.; Li, K.; Pei, L.; Zhu, C. An integrated approach for real-time model-based state-of-charge estimation of lithium-ion batteries. *J. Power Sources* **2015**, *283*, 24–36. [CrossRef]
34. Lee, N.G.; Kim, Y.J.; Kim, W.S.; Kim, Y.S.; Kim, T.J.; Baek, S.M.; Choi, Y.; Kim, Y.K.; Choi, I.S. Study on the Improvement of Transmission Error and Tooth Load Distribution using Micro-geometry of Compound Planetary Gear Reducer for Tractor Final Driving Shaft. *J. Drive Control* **2020**, *17*, 1–12.
35. Park, S.U. *Fatigue Life Evaluation of Spiral Bevel Gear of Transmission Using Agricultural Workload of Tractor*; Chungnam National University: Daejeon, Korea, 2019.
36. Xu, G.; Li, W.; Xu, K.; Song, Z. An Intelligent Regenerative Braking Strategy for Electric Vehicles. *Energies* **2011**, *4*, 1461–1477. [CrossRef]
37. Kim, Y.-J.; Chung, S.-O.; Choi, C.-H.; Lee, D.-H. Evaluation of Tractor PTO Severeness during Rotary Tillage Operation. *J. Biosyst. Eng.* **2011**, *36*, 163–170. [CrossRef]
38. Lee, D.H.; Kim, Y.J.; Chung, S.O.; Choi, C.H.; Lee, K.H.; Shin, B.S. Analysis of the PTO load of a 75 kW agricultural tractor during rotary tillage and baler operation in Korean upland fields. *J. Terramech.* **2015**, *60*, 75–83. [CrossRef]
39. Kim, D.C.; Ryu, I.H.; Kim, K.U. Analysis of tractor transmission and driving axle loads. *Trans. Am. Soc. Agric. Eng.* **2001**, *44*, 751–757.

40. Reddy, G.S.; Narsaiah, J.; Shashikala, G. Dynamic Analysis on Tillage Equipment Used in Agriculture Using Ansys Software. *Int. J. Sci. Res. Sci. Technol.* **2017**, *3*, 890–897.
41. Kim, W.S.; Kim, Y.S.; Kim, T.J.; Park, S.U.; Choi, Y.; Choi, I.S.; Kim, Y.K.; Kim, Y.J. Analysis of power requirement of 78 kW class agricultural tractor according to the major field operation. *Trans. Korean Soc. Mech. Eng. A* **2019**, *43*, 911–922. [CrossRef]